

Article

Interaction of Redox-Active Copper(II) with Catecholamines: A Combined Spectroscopic and Theoretical Study

Miriam Šimunková^{1,*}, Zuzana Barbieriková¹, Milan Mazúr¹ , Marian Valko^{1,2}, Suliman Y. Alomar² , Saleh H. Alwaseel² and Michal Malček¹ 

¹ Department of Physical Chemistry, Institute of Physical Chemistry and Chemical Physics, Faculty of Chemical and Food Technology, Slovak University of Technology, Radlinského 9, 812 37 Bratislava, Slovakia

² Zoology Department, College of Science, King Saud University, Riyadh 11451, Saudi Arabia

* Correspondence: miriama.simunkova@stuba.sk

Abstract: In this work, attention is focused on the non-essential amino acid L-Tyrosine (TYR) hydroxylated to L-DOPA, which is the precursor to the neurotransmitters dopamine, noradrenaline (norepinephrine; NE) and adrenaline (epinephrine; EP) known as catecholamines and their interactions with redox-active Cu(II). Catecholamines have multiple functions in biological systems, including the regulation of the central nervous system, and free (unbound) redox metal ions are present in many diseases with disturbed metal homeostasis. The interaction between catecholamines and Cu(II) has been studied by means of Electron Paramagnetic Resonance spectroscopy (EPR), EPR spin trapping and UV-vis spectroscopy. The obtained spectroscopic results are supported by Density Functional Theory calculations. Only minor qualitative and quantitative changes in the UV-vis spectra of all the studied compounds have been observed following their interactions with Cu(II) ions. The low-temperature EPR spectra were more convincing and confirmed the interaction between Cu(II) ions and all the studied compounds, involving hydroxyl groups and amino nitrogens. The use of an ABTS assay revealed that the compounds under study possessed radical-scavenging activities against ABTS^{•+} in the order TYR < EP < DA < NE~L-DOPA. The neurotransmitters DA, NE and EP, following their interaction with Cu(II), exhibit the ability to (partially) reduce Cu(II) to Cu(I) species which was confirmed using the Cu(I) specific chelator neocuproine. EPR spin-trapping experiments revealed the suppressed formation of hydroxyl radicals (\bullet OH) in a copper(II) catalyzed Fenton-like system in the presence of catecholamines. Only in the case of EP was autooxidation in a stock solution observed. Furthermore, the oxidation of EP is enhanced in the presence of Cu(II) ions. In conclusion, it has been confirmed that the oxidation of catecholamines in the presence of copper promotes the redox cycling process, resulting in the formation of ROS, which may, in turn, cause damage to neuronal systems.

Keywords: catecholamines; copper(II); neurotransmitters; radical-scavenging activity; EPR spectroscopy; spin-trapping; DFT



Citation: Šimunková, M.; Barbieriková, Z.; Mazúr, M.; Valko, M.; Alomar, S.Y.; Alwaseel, S.H.; Malček, M. Interaction of Redox-Active Copper(II) with Catecholamines: A Combined Spectroscopic and Theoretical Study. *Inorganics* **2023**, *11*, 208. <https://doi.org/10.3390/inorganics11050208>

Academic Editor: Dinorah Gambino

Received: 28 March 2023

Revised: 5 May 2023

Accepted: 10 May 2023

Published: 12 May 2023



Copyright: © 2023 by the authors. Licensee MDPI, Basel, Switzerland. This article is an open access article distributed under the terms and conditions of the Creative Commons Attribution (CC BY) license (<https://creativecommons.org/licenses/by/4.0/>).

1. Introduction

The Fenton reaction is considered one of the main sources of damaging hydroxyl radicals that cause damage to all important biomolecules, including DNA [1,2]. In this reaction, hydrogen peroxide, a by-product of cellular respiration, is heterolytically cleaved by the catalytic action of cuprous or ferrous ions [3]. One of the cell types most vulnerable to damage by free radicals is neuronal cells. In fact, DNA damage induced by redox-active metals and redox cycling reactions can lead to neurodegeneration. The consequences of DNA damage-induced apoptosis include greater incidences of neurodegenerative disorders such as Alzheimer's, Parkinson's and Huntington's diseases [4–7].

In this work, our attention is focused on the amino acids L-tyrosine (TYR) and L-DOPA, and the catecholamine neurotransmitters dopamine (DA), norepinephrine (NE; noradrenaline), and epinephrine (EP; adrenaline) presented in Figure 1 playing important roles in the physiological of organisms such as motor function, mood control, anxiety, depression and other functions [8–16]. Their interaction with redox metals has been observed under various pathological states of disturbed metal homeostasis [5,7]. In agreement with this, in this work, we attempt to study the interaction of catecholamines with the redox metal Cu(II) using a variety of spectroscopic techniques.

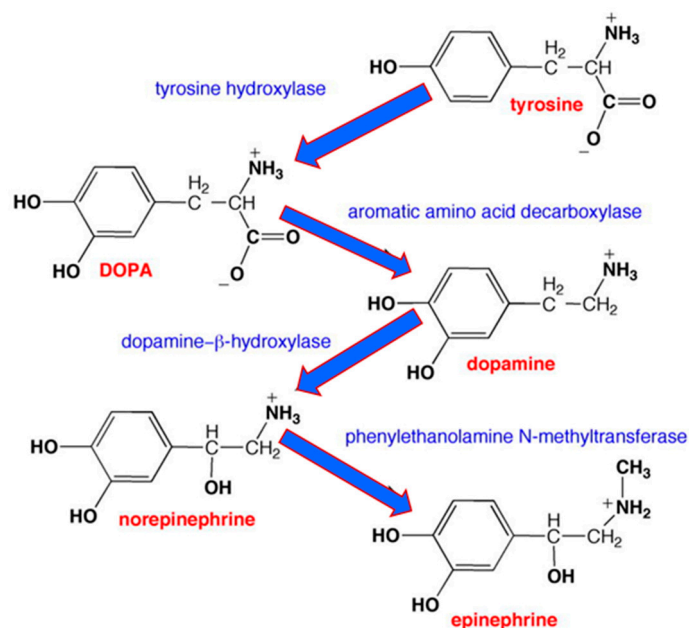


Figure 1. The catecholamine cascade: synthesis of the neurotransmitter epinephrine from tyrosine.

TYR, L-DOPA and catecholamines contain in their structures hydroxyl groups and possess radical scavenging/antioxidant properties and metal chelating properties via carboxylate (L-tyrosine) or hydroxyl groups (DA, EP and NE) or both carboxylate and hydroxyl groups (L-DOPA). The first paper reporting the interaction of Cu(II) ions with catecholamines was published in the early 1960s [17]. The formation of Cu(II) complexes with catecholamines in aqueous solutions has already been reported in 1979 by Fazakerley et al. [18]. Catechol-containing Cu(II) complexes are still extensively studied due to their interesting properties [19–21]. In this paper, the authors, for the first time, propose the reduction of Cu(II) to Cu(I) following the interaction of cupric ions with catecholamines.

In the course of the oxidation of L-DOPA, H_2O_2 is generated and thus may react in Fenton-type reactions, producing damaging hydroxyl radicals ($\bullet\text{OH}$) [22], particularly when metal ions are present. This suggests the neurotoxic effect of L-DOPA in the long-term treatment of PD. Despite the antioxidant properties of catecholamine molecules, under certain unphysiological conditions, such as in the presence of free redox metals involving Cu(II) or Fe(II), they can be involved in redox cycling reactions resulting in reduced forms of metal ions and, secondarily, ROS-inducing DNA damage [23]. In fact, catecholamines can undergo oxidation to form reactive quinones, H_2O_2 and/or $\text{O}_2^{\bullet-}$, a reaction that may occur either spontaneously with molecular oxygen or enzymatic assistance [13,14,24]. A key process promoting the formation of ROS, with a possible consequence in prooxidant effect, appears to be the one-electron reduction of quinones and the subsequent reaction between the formed semiquinone radical and dioxygen [25]. One-electron reduction accompanied by autoxidation and redox cycling in the presence of dioxygen contributes greatly to the toxicity characterizing various quinones, involving also catecholamines [26]. o-Quinones, physiological oxidation products of catecholamines, may

contribute to redox cycling, toxicity and apoptosis, i.e., the neurodegenerative processes underlying PD and schizophrenia [25].

The established link between metal-induced oxidative stress and neurological diseases indicates the importance of studying the interactions of neurotransmitters with copper. We believe that the obtained results will improve our understanding of the mode and nature of Cu's binding with neurotransmitters and the role of Cu in the antioxidant/prooxidant properties of neurotransmitters.

2. Results and Discussion

2.1. Interaction of Catecholamines with Cu(II): A UV-Vis and EPR Spectroscopic Study

UV-vis spectroscopy was used to study aqueous solutions of catecholamines in the presence of Cu(II) ions to observe possible spectral changes due to the chelation of metal ions [27]. UV-vis spectra of colorless catecholamines in aqueous solutions of the studied compounds (Figure 2) exhibit a single absorption band at about 288 nm with no changes in the intensity or position within 30 min. The only exception has been observed for EP, showing weak bands at 330 nm and 460 nm. After the addition of the CuCl₂ solution, a series of spectra of the Cu(II) chelates with catecholamines (at a 1:2 ratio) were recorded within the 30 min periods. Only a small hyperchromic shift was observed in the case of TYR (mild chelating capacity) and L-DOPA. A slight increase in the absorbance intensity can be attributed to extended conjugation upon the coordination of these two catecholamines to Cu(II) ions. In agreement with this, absorption bands became a little broader compared to a system with a lower degree of conjugation. A new peak appears as a shoulder around 305 nm in the cases of DA, NE and EP, suggesting changes in the electronic structure of the corresponding molecules in the presence of Cu(II). An aqueous solution of EP became bright coral-colored with a new absorption peak at 480 nm, which points to the formation of a small amount of EP autooxidation products in the solution [28,29]. Oxidation of EP in the presence of Cu(II) was reported by Balla et al. [30]. Jobs plot experiments have been performed, and results are shown in Figure S5. The results have shown that all neurotransmitters, with the exception of dopamine, coordinate to Cu(II) approximately in stoichiometric ratios of 1:2. Dopamine has been shown to be coordinated to Cu(II) ions approximately in a ratio of 1:1, in agreement with previously published preliminary results [17].

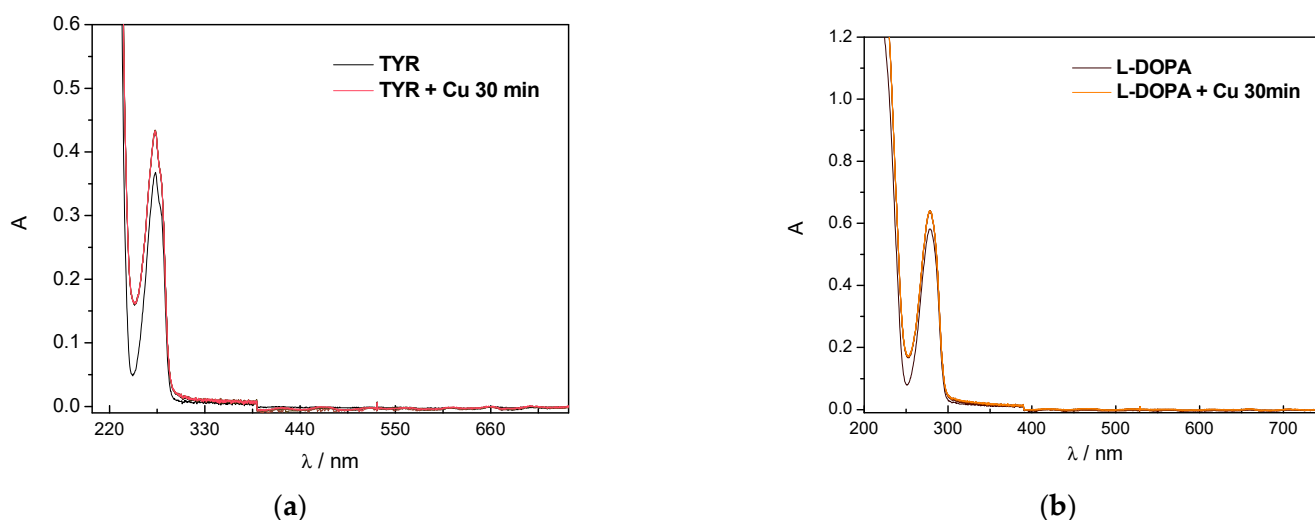


Figure 2. Cont.

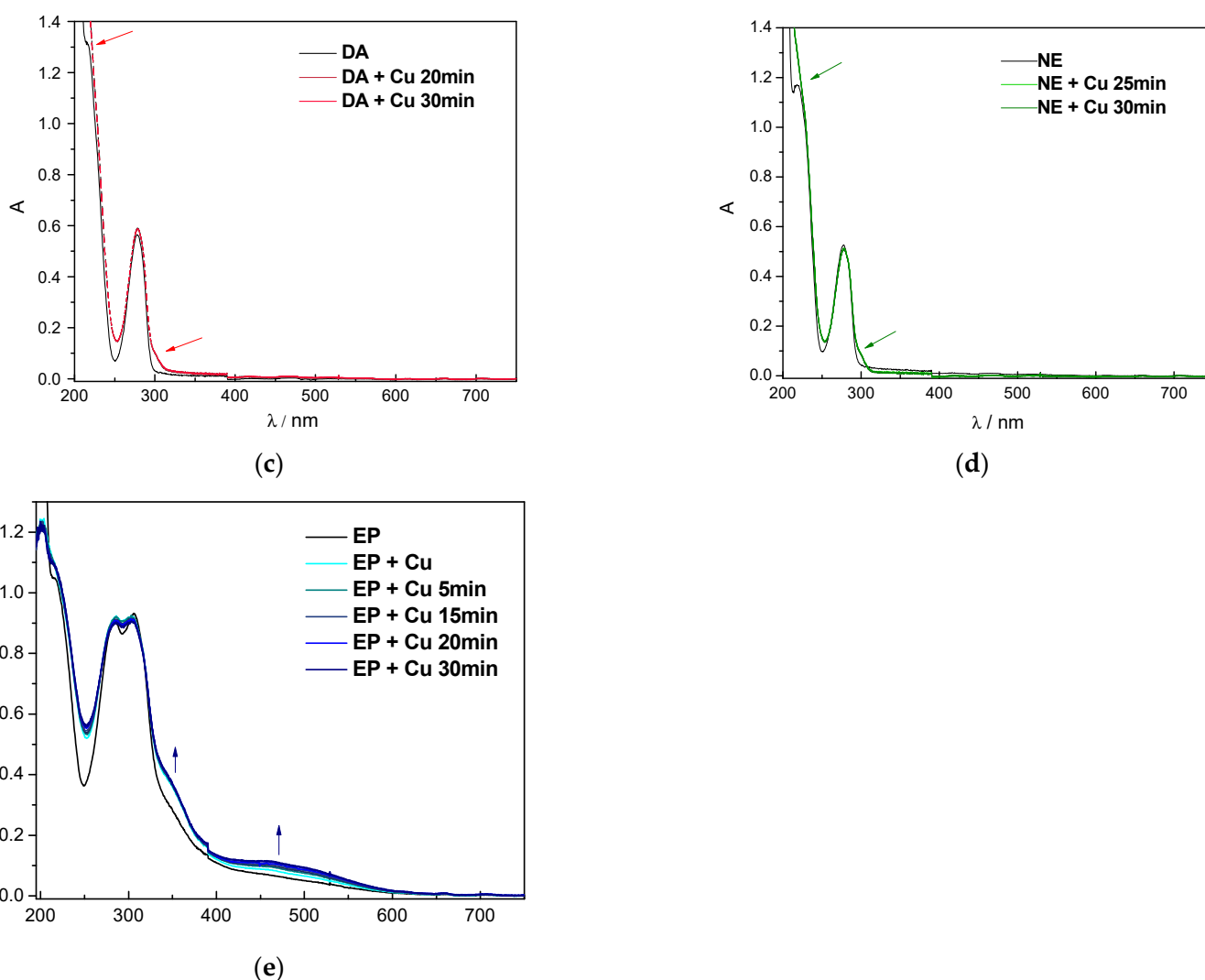


Figure 2. UV/Vis spectra of (a) TYR, (b) L-DOPA, (c) DA, (d) NE and (e) EP ($c(\text{sample}) = 1.5 \times 10^{-5}$ M), and their Cu-catecholamine (1:2) chelates ($c(\text{Cu(II)}) = 7.5 \times 10^{-6}$ M) in MOPS buffer (pH = 7.2).

Fluorescence spectroscopy was applied to measure the emission spectra of the studied compounds before and after the addition of Cu(II). The emission spectra are presented in Figure S6. Decreases in fluorescence intensity in the region from 600–700 nm can be observed in all cases; however, in the case of EP, the decrease in intensity is prominent in the whole measured wavelength region.

Since the UV-vis and emission spectra of Cu(II) and catecholamine interactions provided only limited information, EPR spectroscopy, as a very sensitive technique to characterize the local environment around Cu(II) ions, was used as a complementary technique to ascertain the nature of Cu-catecholamine interactions in greater detail. Since Cu(II) is paramagnetic with one unpaired electron, differences in EPR spectra of catecholamines and Cu(II) compared to the EPR spectrum of CuCl_2 (Figure 3) provide information about changes in the local environment around Cu(II) atoms [31].

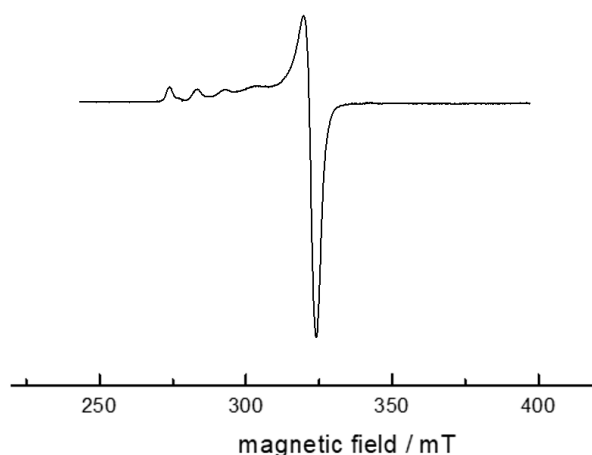


Figure 3. Reference EPR spectrum of CuCl_2 recorded at 77 K.

The EPR spectra of the Cu(II) -complex under study measured at room temperature are poorly resolved, with a poor signal-to-noise ratio (spectra are not shown). A significantly better resolution was achieved by measuring the spectra at 77 K.

The low-temperature (77 K) EPR spectra of the Cu(II) -TYR interaction (1:2) in the MOPS buffer are shown in Figure 4. The spectrum measured 5 min after mixing the stock solution of tyrosine with CuCl_2 solution has typical well-resolved anisotropic features with slight rhombic distortion in g -factors and a well-resolved hyperfine splitting pattern around the parallel component of the g tensor ($g_{\parallel} = 2.263$). The parallel component of hyperfine splitting ($A_{\parallel} = 17.94$ mT), points to the axial symmetry around the paramagnetic copper(II) center of the studied complex. A $g_{\parallel}/A_{\parallel}$ ratio of ~ 126.2 cm points to distorted geometry around Cu(II) ions in the xy plane of the complex. Keeping in mind the structure of tyrosine, the coordination of tyrosine to Cu(II) can most probably be achieved via the carboxylic oxygen or nitrogen atom of the amino group. The resolution of EPR spectra is not satisfactory to assign the donor atoms coordinated to Cu(II) ion. Nitrogen donor atoms coordinated to Cu(II) are magnetically active and may provide additional superhyperfine splitting in the EPR spectra; however, in the recorded spectra, such an interaction was not observed.

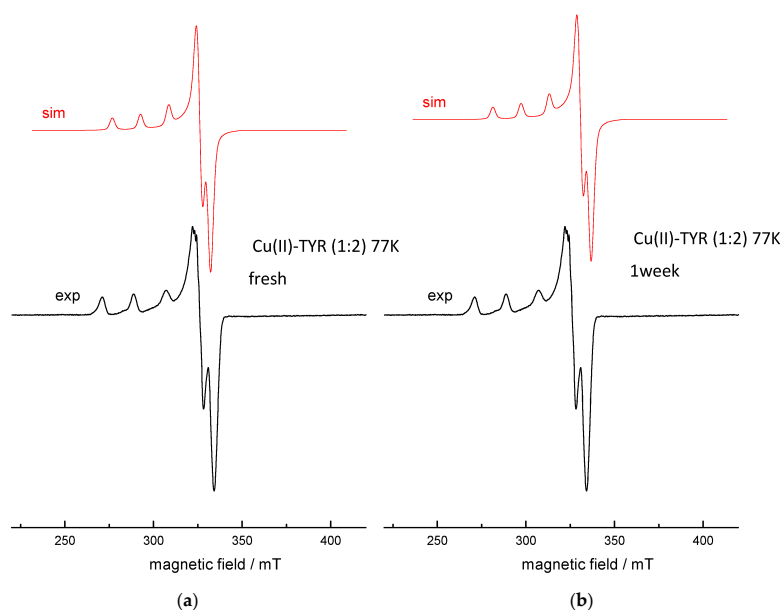


Figure 4. Experimental and simulated EPR spectra of Cu(II) -TYR (1:2) at 77 K, recorded (a) 5 min after mixing and (b) 1 week after mixing.

The prepared system was stored in the dark for 1 week. After 1 week, the same Cu(II)-TYR complex mixture (1:2) was measured. No significant changes in the EPR intensity were observed, as can be seen in Figure 4b. Based on this finding, we can assume that the reduction of Cu(II) to Cu(I) did not occur since no decrease in relative spectral intensity was monitored.

The experimental EPR spectrum of Cu(II)-L-DOPA measured at 77 K using a molar ratio of 1:2 is shown in Figure 5. There are three possible coordination sites of L-DOPA to take into account: (i) the first is the carboxylic group, which becomes deprotonated at pH 7 and thus forms an anionic site (COO⁻), (ii) the second is the two hydroxyl groups of the aromatic ring, which are protonated at pH 7, (iii) and the third possible coordination site is the nitrogen atom. The EPR spectrum presented in Figure 5 suggests the formation of all three abovementioned species, but the abundance of each species is different, as is evidenced by the three different hyperfine splitting sets ($A_{iso,1} = 18.755$ mT; $A_{iso,2} = 16.951$ mT; $A_{iso,3} = 16.797$ mT) with different EPR intensities. The EPR spectrum of the Cu(II)-L-DOPA complex (1:2) was also measured 1 week after mixing. No significant changes were observed; however, small line-broadening occurred in the perpendicular part of the spectrum (spectrum not shown). These changes could be due to the slight variations in equilibrium species over time.

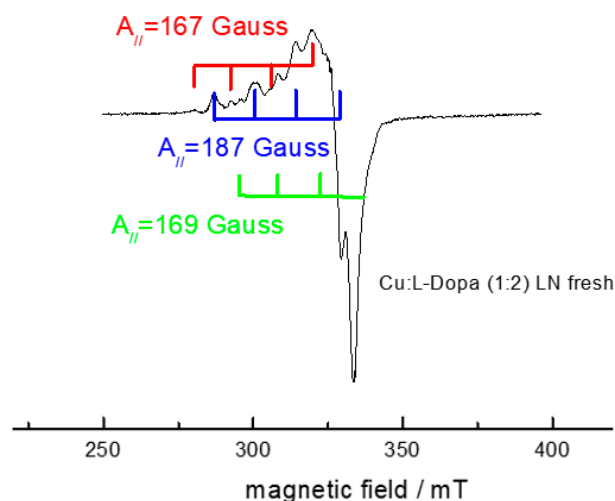


Figure 5. Experimental Cu(II)-L-DOPA (1:2) recorded at 77 K, 5 min after mixing.

EPR spectrum of Cu(II)-DA complex (1:2) measured after mixing at the temperature of liquid nitrogen (77 K) is presented in Figure 6a. The spectrum is quite nicely resolved with values of hyperfine coupling constants $A_{||} = 18.85$ mT, $A_{\perp} = 3.5$ mT and $g_{||} = 2.261$ $g_{\perp} = 2.055$, and low values of spectral linewidth, allowing us to observe a quite rare phenomenon, the signal of both copper isotopes ^{63}Cu and ^{65}Cu , as evidenced by a small set of superimposed splittings in the parallel hyperfine couplings. A $g_{||}/A_{||}$ ratio of 120 cm is rather low and points to a nearly square planar arrangement around Cu(II) ions. The molecular structure of DA offers, at maximum, two binding modes (via both hydroxyl groups or amino nitrogen); thus, we may expect a square planar arrangement around Cu(II) ions due to the coordination of two DA molecules to Cu(II) ion through both hydroxyl groups.

As in the previous cases, we measured the same Cu(II)-DA complex solution (1:2) 1 week after mixing at room temperature and that of liquid nitrogen (Figure 6b). EPR measurements at the temperature of liquid nitrogen (77 K) showed decreased EPR signal intensity, but not as clearly as in the case of room temperature measurement, as presented in Figure S7 in Supplementary material. It is clear that signal intensity is decreased, which suggests that after 1 week, the partial reduction of Cu(II) to Cu(I) has occurred with the logical concomitant oxidation of dopamine.

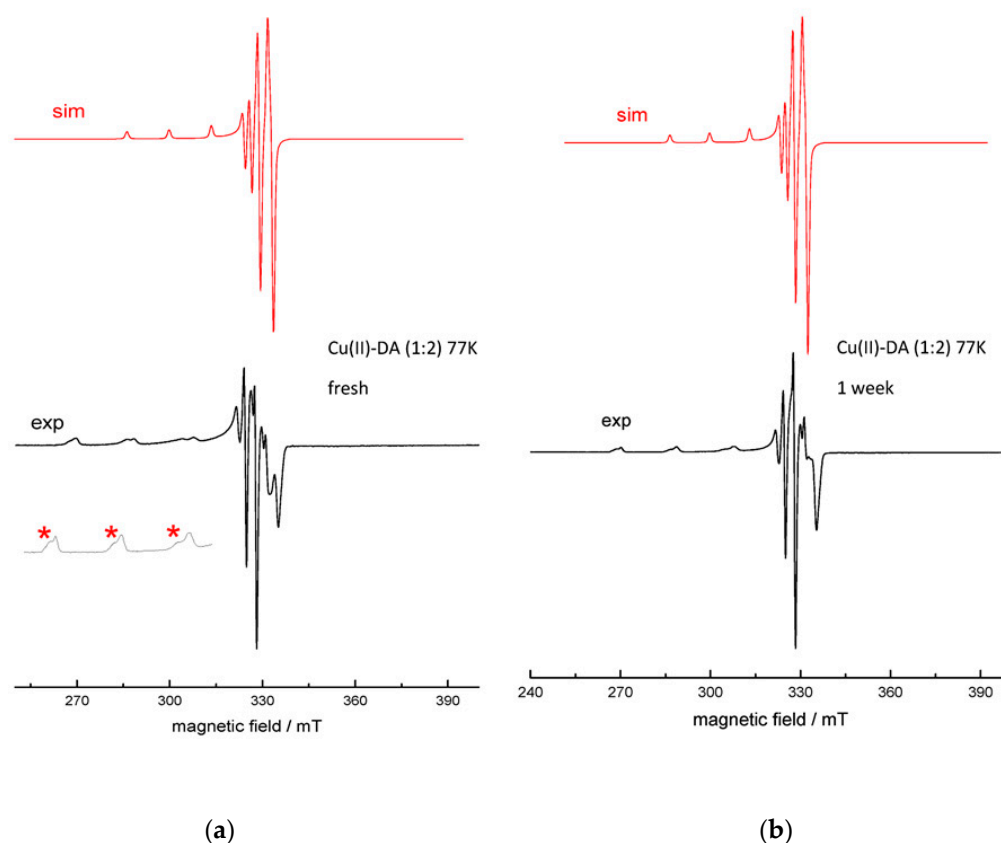


Figure 6. Experimental and simulated EPR spectra of Cu(II)-DA (1:2) recorded at 77 K, recorded (a) 5 min after mixing and (b) 1 week after mixing. Inset: observation of two copper isotopes (^{63}Cu and ^{65}Cu) is highlighted with asterisks.

The EPR spectrum of the Cu(II)-NE complex measured immediately after mixing at RT (not shown) was surprisingly quite nicely resolved, with a hyperfine coupling constant of $A_{\text{iso}}(\text{Cu}) = 3.5$ mT. The EPR spectrum of Cu(II)-NE (1:2) measured at 77 K after mixing is presented in Figure 7. As can be seen from Figure 7, the spectrum is very similar to that of Cu(II)-DA (1:2), with the possible observation of two copper isotopes (^{63}Cu and ^{65}Cu). The similarity of these two spectra can be explained by small differences in the molecular structures of DA and NE (note that norepinephrine has one additional -OH group on the aliphatic side chain). This similarity thus suggests that the -OH group of the side chain does not participate in binding to Cu(II). Therefore, we can assume that, in the case of dopamine and norepinephrine, coordination via the two hydroxyl groups of the aromatic ring is probable. Based on the parameters of the EPR spectrum, a nearly regular square planar arrangement around Cu(II) is adopted after the binding of two catecholamines (see Section 2.4). We note that alternative coordination via the nitrogens of amino groups is also possible (see Section 2.4).

Compared to the EPR spectra measured immediately after mixing, spectra of the Cu(II)-NE (1:2) complex measured after 1 week are clearly less intense, as evidenced by an increased level of noise as well as the decreased resolution of hyperfine coupling structure due to the lower concentration of paramagnetic species in solution. This suggests the reduction of Cu(II) to Cu(I) by coordination of norepinephrine to Cu(II).

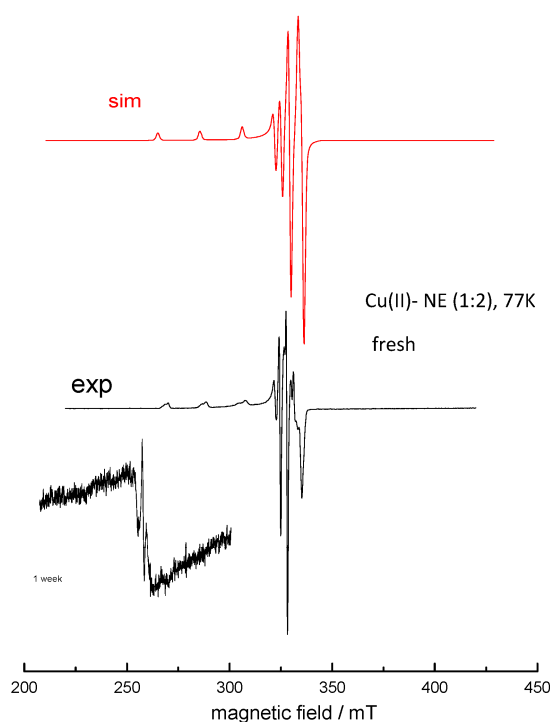


Figure 7. Experimental and simulated EPR spectra of Cu(II)-NE (1:2) recorded at 77 K, 5 min after mixing (inset: spectrum of the same system measured after 1 week).

The catecholamine cascade ends with the formation of epinephrine. The Cu(II)-epinephrine complex was also monitored by EPR spectroscopy. The spectra of the Cu(II)-epinephrine (1:2) system measured 5 min after mixing are presented in Figure 8. The parameters obtained by the simulation ($g_{||}$ 2.262, $A_{||}$ = 18.850 mT), as in previous cases, point to a square planar arrangement since the $g_{||}/A_{||}$ value is 120 cm. The molecular structure of epinephrine differs in the terminal methyl group of the side chain, and there is almost zero probability of binding copper via this methyl group. Thus, it can be assumed that, in the case of EP, Cu(II) is coordinated by two oxygens originating from the hydroxyl groups of the benzene ring with a slightly distorted environment around the Cu(II) ion (see Section 2.4). Alternative coordination via the nitrogen of the amino groups is also possible. Additionally, EPR spectra of complex Cu(II)-epinephrine (1:2) measured after 1 week at room temperature exhibit decreased signal intensity suggesting a mild reduction of Cu(II) accompanied by the oxidation of EP.

To support the theory of the reduction of Cu(II) to Cu(I) following its interaction with dopamine, norepinephrine and epinephrine, UV-vis spectroscopy was used to obtain direct experimental evidence of the presence of Cu(I) species in the reaction mixture. A specific chelator of Cu(I), neocuproine (2,9-dimethyl-1,10-phenanthroline; NC), was added to the corresponding Cu(II) complexes, and the absorption spectra were measured for 90 min. NC, as a specific chelator of Cu(I), is known to form a yellow-colored complex that absorbs light at 450 nm. Figure 9 documents a time-dependent increase of absorption at 456 nm following the mixing of CuCl₂ and selected catecholamines in the presence of the chelator, NC. The formation of a dark yellow complex evidenced by increased absorption at 456 nm confirms that the reduction of Cu(II) to Cu(I) has occurred after its interaction with DA/NE/EP molecules. Logically, the catechol ring is oxidized to its semiquinone form. This observation supports the theory of ROS formation, where Cu(I) serves as a catalytic agent.

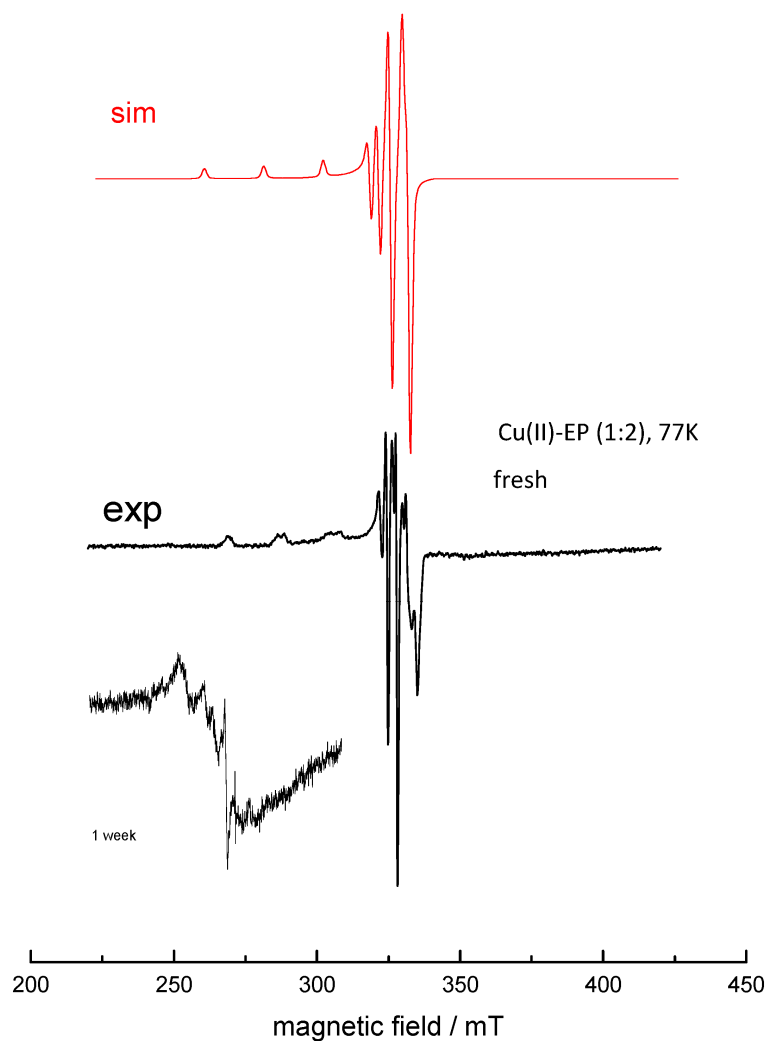


Figure 8. Experimental and simulated EPR spectra of Cu(II)-EP (1:2) recorded at 77 K, 5 min after mixing (inset: measured after 1 week, RT).

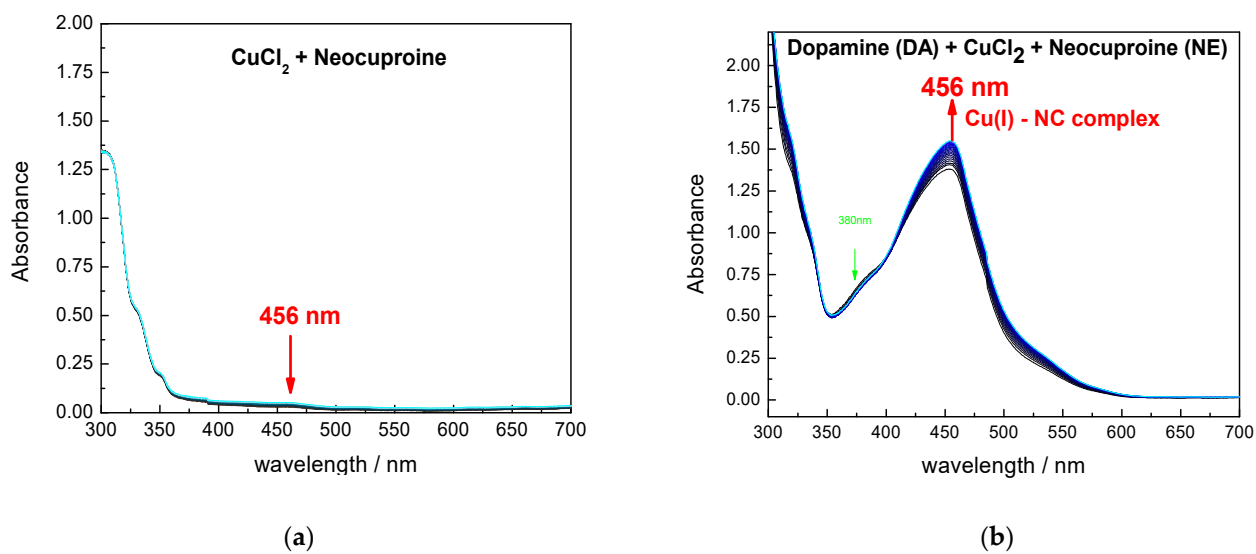


Figure 9. Cont.

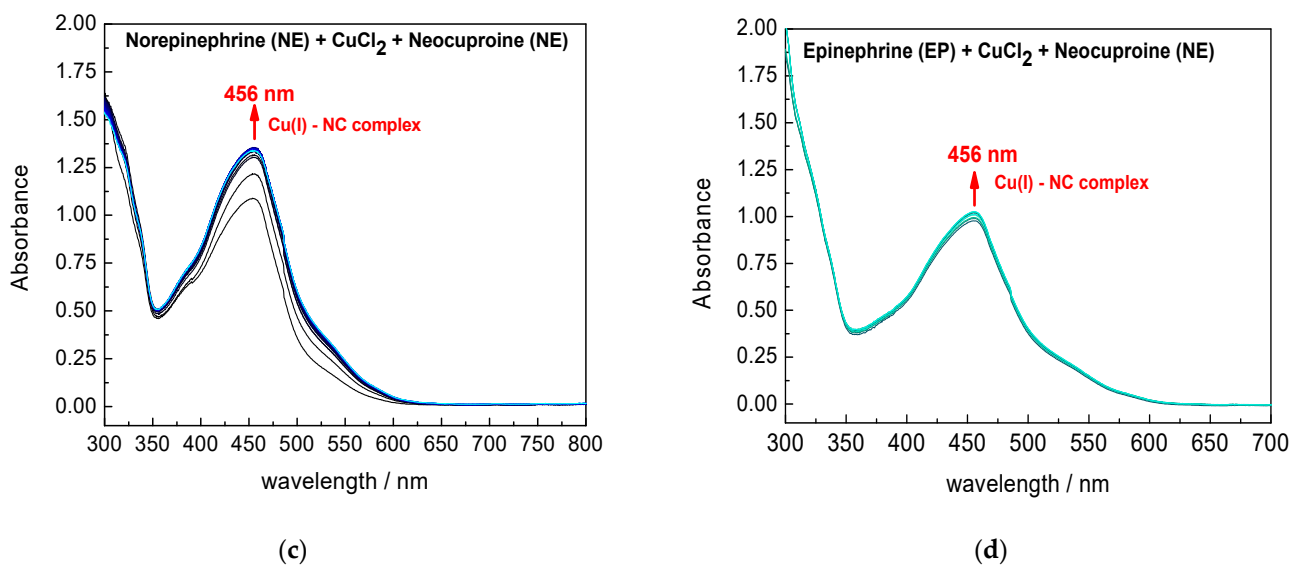


Figure 9. (a) Time-dependent absorption spectra of (a) CuCl_2 ($c_{\text{CuCl}_2} = 1.25 \times 10^{-4}$ M) in the presence of NC ($c_{\text{NC}} = 5 \times 10^{-4}$ M). The very small absorption band at 456 nm reflects only a negligible amount of Cu(I) in the CuCl_2 stock solution. (b–d) Time-dependent (90 min) absorption spectra of system CuCl_2 ($c_{\text{CuCl}_2} = 1.25 \times 10^{-4}$ M) with catecholamine ($c_{\text{sample}} = 2.5 \times 10^{-4}$ M) in water in the presence of NC ($c_{\text{NC}} = 5 \times 10^{-4}$ M). The absorption band at 456 nm shows the time-dependent (90 min) increase of absorbance due to the formation of a Cu(I)–NC complex.

2.2. Radical Scavenging Activity of Catecholamines and Their Cu(II) Complexes

It is well known that catecholamines and the metabolites of dopamine are excellent radical scavengers [32–34]. For example, the hydroxyl radical scavenging capacity of DA, EP and NE reported earlier ranges from 62% to 89% [33], while superoxide anion radical capacity of the same set of catecholamines is within the range of 67–73% [34]. In our study, $\text{ABTS}^{\bullet+}$ assay was used to evaluate the radical scavenging properties of studied compounds alone and in the presence of Cu(II) ions. The results of the $\text{ABTS}^{\bullet+}$ test are presented in Table 1. We can assume that all compounds under study exhibit quite good radical scavenging activities and inhibit $\text{ABTS}^{\bullet+}$ absorbance in the range of 32–99%. The ability to scavenge $\text{ABTS}^{\bullet+}$ radical cations increases in the order: $\text{TYR} < \text{EP} < \text{DA} < \text{NE} \sim \text{L-DOPA}$. The results are summarized in Table 1 as the percentage of inhibition of $\text{ABTS}^{\bullet+}$ absorbance. Differences in radical-scavenging properties are clear and lie in the different molecular structures of catecholamine ligands. The most active compounds from the group of catecholamines are L-DOPA and NE. Both compounds caused more than a 90% decrease in $\text{ABTS}^{\bullet+}$ absorbance. On the other hand, the radical-scavenging activity of amino acid TYR is rather small when compared to other catecholamine compounds. Such an observation was expected since TYR contains only one hydroxyl group, the most potent functional group from the viewpoint of radical scavenging activity. After the formation of complex compounds with Cu(II), only a very small effect on the inhibition % was observed. In the second series, the water solution of CuCl_2 was mixed with the solution of the studied compound 24 h prior to the test. Only negligible changes compared to the fresh mixtures were observed, as presented in Table 1.

Table 1. Scavenging activity of $\text{ABTS}^{\bullet+}$ by studied compounds alone and in the presence of Cu expressed as inhibition of $\text{ABTS}^{\bullet+}$ absorbance in %.

$\text{ABTS}^{\bullet+}$ INH/%	TYR	L-DOPA	DA	NE	EP
catecholamine	33	96	74	92	37
+ Cu(II) fresh	36	97	75	93	36
+ Cu(II) 24 h	32	99	77	94	55

Surprisingly, different radical scavenging activity was observed in the case of EP. Very inconsistent activity may be caused by the autooxidation of epinephrine in aqueous solutions to its quinone form. Thus, antioxidant capacity is limited only to the non-oxidized moiety of EP present in the stock solution. Additionally, it has been demonstrated that adrenochrome, the oxidation product of EP, promotes a redox cycling process with the production of superoxide anions and hydrogen peroxide [35].

2.3. EPR Spin-Trapping Study of Catecholamines under the Conditions of Fenton Reaction

To complement the above-discussed findings, further investigation was performed using the EPR spin-trapping technique to ascertain the effect of catecholamines and their precursor tyrosine on the formation of radical species in a model copper Fenton-system (e.g., $\bullet\text{OH}$ and $\text{O}_2^{\bullet-}$, containing the CuCl_2 dissolved in water and H_2O_2). The reactive radicals generated after the initiation of the reaction by hydrogen peroxide were monitored by employing the DMPO spin-trapping agent. The time course of EPR spectra obtained in the reference system over time (the first spectrum was acquired 120 s after the addition of H_2O_2) is shown in Figure 10 and represents the four lines of the stable EPR signal even after 10 min. The signal can be unequivocally attributed to the $\bullet\text{DMPO-OH}$ spin adduct ($a_N = 1.486$ mT, $a_{H\beta} = 1.438$ mT; $g = 2.0057$). The dominant trapping of hydroxyl radicals in analogous copper-based reference Fenton systems has been reported previously [36]. The addition of the studied catecholamines to the system affected the EPR signal intensity time profile rather than the character of the EPR signals observed. $\bullet\text{DMPO-OH}$ spin adduct was monitored in the system containing all studied compounds; however, the signal intensity varies significantly. The most intense decrease in the EPR signal intensity over the whole monitored time period was observed for L-DOPA (Figures 10 and 11). The presence of DA and NE in the model Fenton system resulted in the suppressed EPR signal intensity, which continued to decrease over time (Figures 10 and 11). Conversely, in the case of TYR, where the initially-recorded signal (120 s after the addition of H_2O_2) was rather low, comparable to the L-DOPA experiment, over time, the intensity increased, almost reaching the intensity of the pure model system after 10 min.

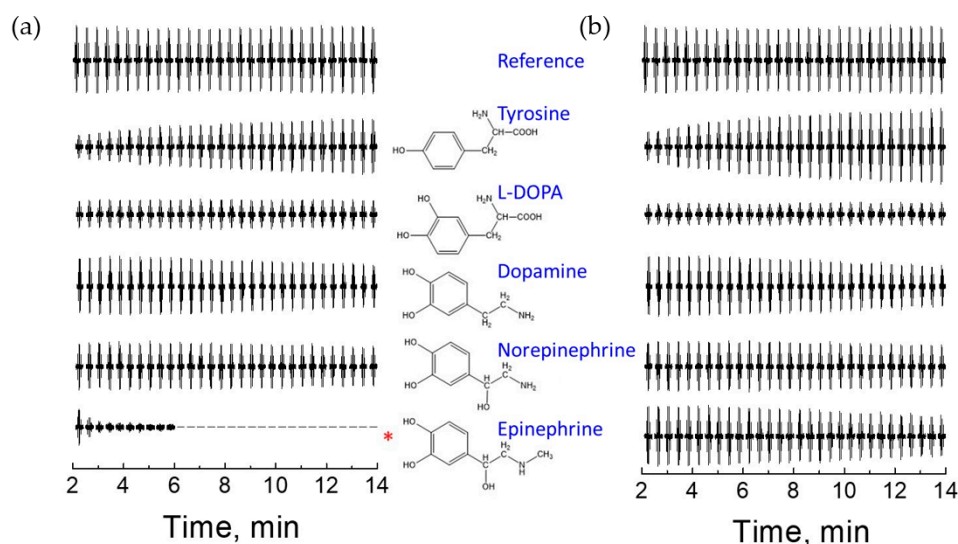


Figure 10. Set of experimental EPR spectra of $\bullet\text{DMPO-OH}$ obtained after the addition of hydrogen peroxide to the (a) aqueous solution of CuCl_2 , H_2O /aqueous solution of studied compound (1:2) containing a DMPO spin-trapping agent. (b) An aqueous solution of CuCl_2 mixed with an aqueous solution of the studied compound (1:2) 24 h prior to measurement, containing a DMPO spin-trapping agent. Initial concentrations: $c(\text{CuCl}_2) = 2$ mM; $c(\text{CuCl}_2) = 1$ mM; $c(\text{DMPO}) = 0.02$ M; $c(\text{H}_2\text{O}_2) = 0.01$ M. (* points on the unusual behavior of EP).

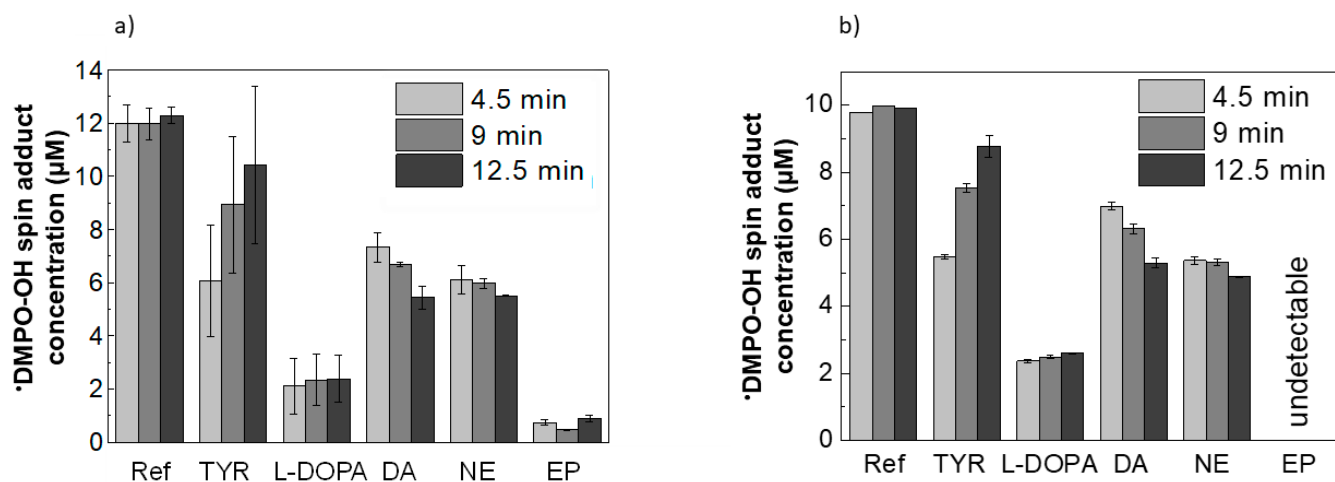


Figure 11. The total concentration of \bullet DMPO-OH spin adducts evaluated from the double-integrated EPR spectra measured in (a) aqueous solution of CuCl_2 (Ref) and aqueous solutions of studied compounds/containing a DMPO spin-trapping agent after the addition of hydrogen peroxide. (b) An aqueous solution of CuCl_2 (Ref) and aqueous solutions of CuCl_2 mixed with an aqueous solution of studied compounds (1:2) 24 h prior to measurement, containing a DMPO spin-trapping agent 2 min after the addition of hydrogen peroxide. In the case of EP, the concentration of the spin adduct was undetectable. Initial concentrations: $c(\text{CuCl}_2) = 2 \text{ mM}$; $c(\text{CuCl}_2) = 1 \text{ mM}$; $c(\text{DMPO}) = 0.02 \text{ M}$; $c(\text{H}_2\text{O}_2) = 0.01 \text{ M}$.

To follow the time effect of the interaction between the catecholamines and copper cations observed in the EPR experiments presented above, the samples were mixed with CuCl_2 24 h prior to the measurement. Interestingly, no impact on the character or intensity of the observed EPR signals was observed, as shown in Figure 10b, the only exception being EP.

As shown above, the EP molecule behaves rather differently compared to other studied compounds, which can also be seen by the EPR spin-trapping experiments in the model Fenton system. When the EP solution is mixed with the CuCl_2 directly before the measurement, the addition of H_2O_2 leads to the generation of the EPR spectrum containing two species. While at the beginning of the measurement (120 s after the addition of H_2O_2) \bullet DMPO-OH adduct dominates the spectrum (Figure 10), another EPR signal attributed to the spin-trap oxidation product \bullet DMPO-X starts to dominate within the next few minutes (Figure 11). The ratio of these two signals continues to change over time, and after 15 min, the \bullet DMPO-OH dominates the spectrum again. This suggests the rather complex redox behavior of EP and its involvement in the ongoing reactions primarily originating from the Fenton system. An analogous experiment performed with the EP solution mixed with CuCl_2 24 h prior to the measurement shows the time course of the \bullet DMPO-OH EPR signal comparable to DA. This significant change in behavior can be linked with the EP oxidation in water solution over time due to the interaction with copper cations.

2.4. DFT Calculations

For the sake of comparison to the above-reported experiments, the Cu(II)-catecholamine complexes with ligand: Cu molar ratio of 2:1 have to be considered. The optimized structures of the particular Cu(II)-catecholamine complexes (molar ratio 1:2), including their spin density distributions, are shown in Figure 12. The calculated average Cu-O and Cu-N bond distances, the corresponding delocalization indices (DIs) and the QTAIM charge and spin densities on the Cu atom are compiled in Table 2. The Cu(II) ions coordinated via the oxygens of the hydroxyl groups (O,O-Cu-O,O) in Cu-LDOPA, Cu-DA, Cu-NE and Cu-EP adopt square planar coordination polyhedrons, Figure 12 (left panel), which is in agreement with measured EPR spectra. In the case of Cu(II) coordination via nitrogens

of the amino groups (N-Cu-N), the optimized N-Cu-N angle is nearly linear, within the range of 174–179°. The calculated Cu-O and Cu-N bond distances are approximately 1.97 and 1.91 Å, respectively. The corresponding DI values are around 0.4 and 0.6, respectively, pointing to the formation of coordination bonds between the Cu(II) ion and interacting catecholamines. Note that the DI value is a measure of the number of shared electrons between the two atoms, i.e., the DI value of 1.0 corresponds to a single covalent bond [37]. For completeness, detailed QTAIM bond characteristics of Cu-O and Cu-N bonds of the studied complexes are shown in Supplementary material (Table S1).

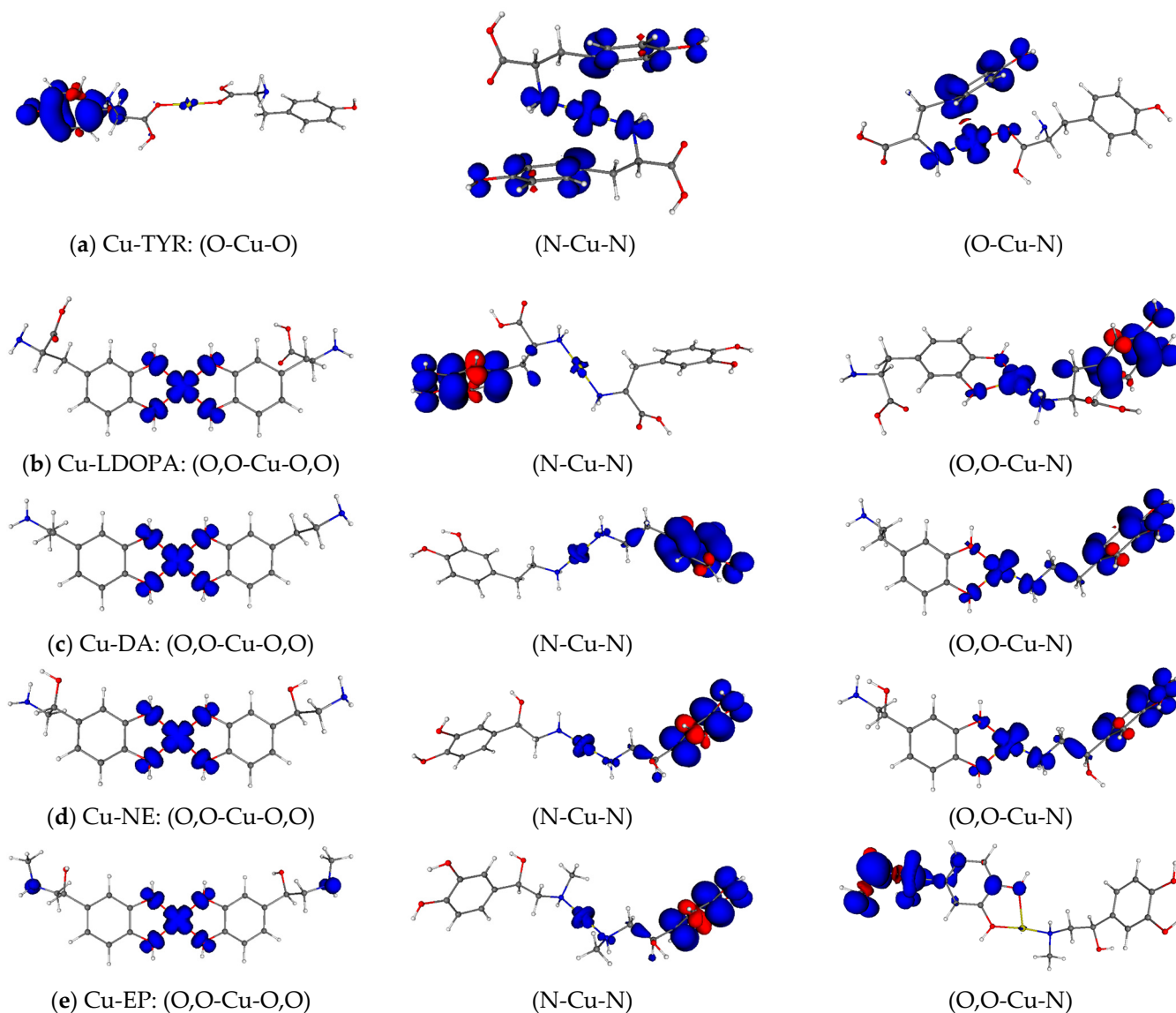


Figure 12. B3LYP/6-311G* spin density distribution of the studied Cu-complexes (molar ratio 1:2). The isovalue was set to ± 0.002 .

Table 2. Calculated B3LYP/6-311G* Cu-O, Cu-N bond distances, QTAIM charges and spin densities on Cu atom, and the Cu oxidation state in the studied complexes (Ligand: Cu molar ratio is 2:1). (X = O, N).

Complex	Binding	d(Cu-X)/Å	DI(Cu-X)/-	q(Cu)/e	Spin(Cu)/e	Cu Oxidation State
Cu-TYR ^a	O-Cu-O ^a	1.86 ^a	0.52 ^a	0.80 ^a	0.01 ^a	Cu(I)
	N-Cu-N	1.96	0.55	0.97	0.48	Cu(I-II)
	O-Cu-N	1.91 ^b , 1.93 ^c	0.45, 0.59 ^c	1.06	0.50	Cu(I-II)
Cu-LDOPA	O,O-Cu-O,O	1.97	0.38	1.40	0.74	Cu(II)
	N-Cu-N	1.91	0.62	0.67	0.02	Cu(I)
	O,O-Cu-N	1.96 ^b , 1.94 ^c	0.38 ^b , 0.58 ^c	1.00	0.35	Cu(I-II)
Cu-DA	O,O-Cu-O,O	1.96	0.39	1.40	0.74	Cu(II)
	N-Cu-N	1.91	0.63	0.70	0.07	Cu(I)
	O,O-Cu-N	1.96 ^b , 1.92 ^c	0.37 ^b , 0.61 ^c	1.09	0.44	Cu(I-II)
Cu-NE	O,O-Cu-O,O	1.96	0.39	1.40	0.75	Cu(II)
	N-Cu-N	1.91	0.63	0.72	0.10	Cu(I)
	O,O-Cu-N	1.95 ^b , 1.91 ^c	0.37 ^b , 0.62 ^c	1.14	0.50	Cu(I-II)
Cu-EP	O,O-Cu-O,O	1.98	0.37	1.36	0.70	Cu(II)
	N-Cu-N	1.92	0.60	0.72	0.09	Cu(I)
	O,O-Cu-N	1.92 ^b , 1.91 ^c	0.42 ^b , 0.62 ^c	0.73	0.00	Cu(I)

^a coordination via the oxygens of COOH groups. ^b Cu-O bond. ^c Cu-N bond.

Besides the structural parameters, the ability of the studied catecholamines to reduce Cu(II) to Cu(I) is inspected via QTAIM analysis. The oxidation state of the particular atom in the molecule can be computationally determined using several different quantities [38]. In our case, the formal oxidation state of Cu in the studied complexes can be (in a brute-force way) estimated via the value of the QTAIM spin density of the Cu atoms. In particular, spin densities close to zero indicate the transfer of the unpaired electron from the Cu(II) ions to the catecholamine moiety (i.e., the oxidation of the catecholamine molecule). As can be seen from Table 2, in the case of N-Cu-N coordination, the spin density on Cu is lower than 0.1 e in all studied systems except Cu-TYR. This result points to the ability of L-DOPA, DA, NE and EP to reduce the Cu(II) to Cu(I) when they are coordinated to Cu via the nitrogens of amino groups, see Figure 12 (right panel). On the other hand, when these species (L-DOPA, DA, NE and EP) are coordinated to Cu via the oxygens of the hydroxyl groups (O,O-Cu-O,O), the unpaired electron remains localized mostly on the Cu atom (around 0.7 e) and the coordinating oxygens, see Figure 12 (left panel). Herein, the reduction of Cu(II) to Cu(I) does not occur. The preferred oxidation states of Cu in all the studied complexes (2:1) are compiled in Table 2. In the cases of Cu-TYR, Cu-LDOPA, Cu-DA and Cu-NE coordinated to one ligand via the hydroxyl groups and the second one via the nitrogen group (O,O-Cu-N), only the partial reduction of Cu occurs (the spin density on Cu is around 0.4 e). These complexes are denoted as “Cu(I-II)” in Table 2. For illustration, the spin density distributions of the studied Cu-complexes are visualized in Figure 12.

3. Experimental

Powdered samples of studied compounds in their L-form (tyrosine, L-dihydroxyphenylalanine, dopamine hydrochloride, norepinephrine hydrochloride, epinephrine hydrochloride), MOPS buffer (pKa = 7.2), DMPO and TEMPOL were purchased from Sigma – Aldrich co. CuCl₂ × 2 H₂O and NaOH were purchased from Merck. Neocuproine was obtained from Alfa Aesar. All chemicals were of analytical quality grade.

3.1. Spectroscopic Study

3.1.1. UV-Vis Spectroscopy

The UV-Vis spectra of the studied catecholamines were measured using a UV-Vis-NIR spectrometer (Shimadzu UV3600, Kyoto, Japan). The concentration of stock solutions of all studied compounds was 1 mM. Spectra were measured for 30 min at room temperature in quartz cuvettes containing 300 μL of catecholamine stock solution and 150 μL of CuCl_2 stock solution filled with MOPS buffer to a final volume of 2 mL. A 2:1 molar ratio was utilized due to a tendency to precipitation in the 1:1 solutions. To determine the metal:ligand ratio of the formed complexes, Job's method was used. The experiment was performed at room temperature by measuring the spectra of mixtures containing different Cu(II) and ligand (aminoacid/catecholamine) fractions. The emission spectra of the studied systems were measured using a Cary Eclipse Fluorescence spectrometer. Spectra were measured in 3 mL quartz cuvettes at room temperature. The concentrations of the compounds used were: $c(\text{sample}) = 2 \times 10^{-5} \text{ M}$, $c(\text{CuCl}_2) = 1 \times 10^{-5} \text{ M}$.

The possible reduction of Cu(II) to Cu(I) ions upon forming complexes with catecholamines was demonstrated by means of UV-Vis spectroscopy using specific Cu(I)-chelating agent 2,9-dimethyl-1,10-phenanthroline, neocuproine (NC). Samples were prepared by mixing water solutions as follows: 250 μL $\text{CuCl}_2 \times 2 \text{ H}_2\text{O}$ (1 mM), 500 μL studied catecholamine (1 mM), 750 μL deionized water and 500 μL neocuproine (2 mM). Immediately after the addition of NC, the absorption spectra were recorded in quartz cuvettes for 90 min using a Shimadzu UV/vis-NIR spectrometer.

3.1.2. EPR Spectroscopy

Copper binding to catecholamines was examined using spectroscopic methods. EPR spectra were measured using an EPR spectrometer Bruker EMX+ operating at X-band frequencies. The samples were measured as liquid solutions (pH = 7) at room temperature and frozen solutions at the temperature of liquid nitrogen (77 K). $\text{CuCl}_2 \times 2 \text{ H}_2\text{O}$ and catecholamine ligands were dissolved in MOPS buffer with a final concentration of 1 mM. MOPS is capable of buffering solutions within a pH of 6.5–7.9 without any significant interaction with metal ions [39,40]. The solutions were mixed using a molar ligand:Cu ratio of 2:1 and left for 5 min and 1 week, respectively. The spectra were measured in thin capillaries incorporated in Dewar flasks.

3.2. Radical Scavenging Activity

ABTS $^{\bullet+}$ assay: Radical scavenging properties of studied catecholamines and their Cu(II) complexes were monitored via the time-decay of the absorption band at 730 nm of stable radical cations of ABTS (2,2'-azino-bis(3-ethylbenzothiazoline-6-sulphonic acid)) present in the mixture. At first, to form an ABTS $^{\bullet+}$ solution, 3.3 mg of potassium persulfate and 17.2 mg of ABTS were dissolved in 5 mL of deionized water. The prepared solution was left in the dark for 24 h to achieve complete oxidation of ABTS to its radical cation ABTS $^{\bullet+}$. The working solution of ABTS $^{\bullet+}$ was prepared by diluting 0.5 mL of oxidized ABTS $^{\bullet+}$ solution with 30 mL of deionized water. For each measurement, 1700 μL mL of ABTS $^{\bullet+}$ working solution was added to a quartz cuvette containing 50 μL of tested compound (1 mM) and 250 μL of deionized water/225 μL of deionized water + 25 μL of CuCl_2 water solution (1 mM) to achieve molar ratio ligand: Cu = 2:1. The time-decay of absorbance at a wavelength of 730 nm was monitored for 900 seconds. The ABTS $^{\bullet+}$ inhibition percentage was calculated as follows:

$$\text{Inhibition \%} = 100 \times (A_0 - A) / A_0 \quad (1)$$

where A_0 represents the absorbance of the control (pure ABTS $^{\bullet+}$ solution), and A represents the absorbance of the sample (free catecholamine or catecholamine in the presence of Cu(II) ions), respectively.

3.3. EPR Spin-Trapping

The EPR spin-trapping experiments were performed in deionized water using a 5,5-dimethyl-1-pyrrolineN-oxide (DMPO, distilled prior to the application) spin-trap. The model copper-based Fenton system consisted of (a) a copper(II) chloride (1 mM) and H₂O (reference)/water solution of the studied compound, (b) a copper(II) chloride (1 mM) and H₂O (reference)/mixture of water solutions in a CuCl₂:studied compound ratio of 1:2 (mixed 16 h prior to measurement). The EPR spectra were recorded 2 min after the addition of initiator H₂O₂ (0.1 M). The experiments were carried out in triplicate under identical experimental conditions. The concentrations of the spin adducts were determined by the double integration of the EPR spectra with respect to the 4-hydroxy-2,2,6,6-tetramethylpiperidine-N-oxyl (Tempol) calibration curve measured under the same experimental conditions. The experimental EPR spectra were analyzed using the Bruker software WinEPR suite, and the simulation of experimental spectra was performed using the EasySpin 5.2.28 simulation toolbox [41] working under Matlab R2021b software.

3.4. Theoretical Calculations

Geometry optimizations of all studied systems were performed at the B3LYP [42–45]/6-311G(d) [46–48] level of theory in the Gaussian16 program package [49]. The energy-based criterion of the SCF convergence was set to 10^{−8} Hartree. Note that in some cases, quadratically convergent (QC) SCF procedures [50] had to be employed to achieve the desired convergence criteria. All systems containing Cu(II) ions were treated as doublets using the unrestricted Kohn–Sham formalism. Vibrational analysis was employed to confirm that the optimal geometries corresponded to energy minima (i.e., there were no imaginary vibrations). Solvent effects in water were treated via the Polarizable Continuum solvent Model (PCM) [51,52] as implemented in the Gaussian16 package. Quantum theory of atoms in molecules (QTAIM) analysis [53] was performed in the AIMAll package [54] using the Gaussian16 checkpoint files to evaluate the charge density distribution and character of the newly formed Cu–O and Cu–N bonds. QTAIM analysis is a useful tool to obtain insight into the nature of interatomic interactions [55]. Visualization of the optimized structures was performed using the Molekel software suite [56].

4. Conclusions

In this work, we present the results of a combined spectroscopic and theoretical study of the interaction between copper and catecholamines.

Low-temperature EPR spectra, as well as the DFT calculations, confirmed the interaction of Cu(II) ions with the studied ligands (catecholamines). Spin Hamiltonian parameters of the EPR spectra unequivocally confirmed that the catecholamines bind to Cu(II) ion. The EPR spectroscopy of identical mixtures prepared 1 week prior to measurement showed decreased signal intensity, most probably due to the mild reduction of paramagnetic Cu(II) ion with silent EPR Cu(I) species. The Cu(II)-catecholamine interaction was also monitored using UV-Vis spectroscopy; however, only small changes after mixing with CuCl₂ were recorded for all compounds except EP. The spectroscopic study of EP confirmed the presence of an oxidation process that is enhanced in the presence of Cu(II) ions.

Reduction of Cu(II) to Cu(I) in the studied systems was confirmed by UV-Vis spectroscopy using a specific Cu(I) chelator neocuproine, as well as by the theoretical calculations (in particular, spin density distributions calculated using QTAIM analysis).

Radical scavenging activity was monitored using ABTS radical cation assay and via the EPR spin-trapping technique using a DMPO spin-trap in a model Cu-catalyzed Fenton system. All the compounds under study possessed radical-scavenging activity against ABTS^{•+} in the order TYR < EP < DA < NE~L-DOPA. The formation of hydroxyl radicals in a Fenton-like system was decreased in the presence of studied compounds in the order TYR < DA < NE < L-DOPA. In the case of EP, autoxidation in stock solution was observed, and thus, the redox properties of the Cu(II)-EP complex were different from those of the

other complexes under study. Furthermore, the oxidation of EP is enhanced in the presence of Cu(II) ions, which may lead to the formation of toxic quinone species.

In conclusion, the oxidation of catecholamines, serving as neurotransmitters, in the presence of cupric ions promotes a redox cycling process with the production of superoxide anion radicals and hydrogen peroxide. Thus, the redox cycling of copper ions in studied systems may lead to the increased production of damaging radicals such as $\bullet\text{OH}$, which may, in turn, cause damage to neuronal systems. Furthermore, when the catecholamine molecule is rapidly oxidized, its antioxidant capacity is markedly reduced.

Supplementary Materials: The following supporting information can be downloaded at: <https://www.mdpi.com/article/10.3390/inorganics11050208/s1>. Figure S1: Scavenging of $\text{ABTS}^{\bullet+}$ by studied compounds and their Cu(II) complexes (fresh); Figure S2: EPR spectra of $\bullet\text{DMPO-OH}$ and $\bullet\text{DMPOX}$ measured with starting acquisition 2 min after the addition of hydrogen peroxide to aqueous solution of CuCl_2 + EP containing DMPO spin trapping agent; Figure S3: Optimized B3LYP/6-311G* structures of the studied Cu-complexes (molar ratio 1:2), including calculated Cu-O and Cu-N bond distances; Table S1: Calculated B3LYP/6-311G* Cu-O, Cu-N bond distances, and corresponding QTAIM characteristics of the studied complexes (Cu: Ligand molar ratio is 1:2); Figure S4: UV-VIS spectrum of CuCl_2 reference system, $c\text{CuCl}_2 = 7.5 \times 10^{-6}$ M; Figure S5: Job's plots of studied compounds (a) TYR (b) L-DOPA (c) DA (d) NE (e) EP and CuCl_2 Absorption spectra were measured in various molar ratios; Figure S6: Emission spectra of studied compound before (black line) and after addition of CuCl_2 (blue line) in water. Concentration of studied compounds: $c_{\text{sample}} = 2 \times 10^{-5}$ M, $c_{\text{copper(II) chloride}} = 1 \times 10^{-5}$ M; Figure S7: EPR spectrum of Cu(II)-DA (1:2) complex at room temperature immediately after mixing (black line) and after one week (blue line).

Author Contributions: Conceptualization, M.Š. and M.V.; methodology, M.Š., Z.B. and M.V.; validation, S.H.A. and S.Y.A.; formal analysis, M.Š., Z.B., M.M. (Milan Mazúr) and M.M. (Michal Malček); investigation, M.Š., Z.B., M.M. (Milan Mazúr) and M.M. (Michal Malček); resources, M.V.; data curation, M.M. (Michal Malček); writing—original draft preparation, M.Š. and M.M. (Michal Malček); writing—review and editing, M.M., Z.B. and M.V.; project administration, M.V., S.H.A. and S.Y.A.; funding acquisition, M.V. All authors have read and agreed to the published version of the manuscript.

Funding: This work received financial support from Slovak Grant Agencies APVV (contracts APVV-19-0087, APVV-19-0024 and APVV-20-0213) and VEGA (contracts No. 1/0139/20 and 1/0482/20). M.M. (Michal Malček) is also grateful to the HPC center at the Slovak University of Technology in Bratislava, which is a part of the Slovak Infrastructure of High-Performance Computing (SIVVP project, ITMS code 26230120002, funded by the European regional development fund) for the computational time and resources made available. The authors are greatly indebted to all financing sources. S.Y.A. thanks KSU for the DSF Program.

Data Availability Statement: Data will be made available upon request.

Conflicts of Interest: The authors declare that they have no conflict of interest.

References

1. Winterbourn, C.C. Toxicity of iron and hydrogen peroxide: The Fenton reaction. *Toxicol. Lett.* **1995**, *82*, 969–974. [[CrossRef](#)]
2. Thomas, C.; Mackey, M.M.; Diaz, A.A.; Cox, D.P. Hydroxyl radical is produced via the Fenton reaction in submitochondrial particles under oxidative stress: Implications for diseases associated with iron accumulation. *Redox Rep.* **2009**, *14*, 102–108. [[CrossRef](#)] [[PubMed](#)]
3. Ramalingam, M.; Kim, S.J. Reactive oxygen/nitrogen species and their functional correlations in neurodegenerative diseases. *J. Neural Transm.* **2012**, *119*, 891–910. [[CrossRef](#)] [[PubMed](#)]
4. Thanan, R.; Oikawa, S.; Hiraku, Y.; Ohnishi, S.; Ma, N.; Pinlaor, S.; Yongvanit, P.; Kawanishi, S.; Murata, M. Oxidative stress and its significant roles in neurodegenerative diseases and cancer. *Int. J. Mol. Sci.* **2014**, *16*, 193–217. [[CrossRef](#)] [[PubMed](#)]
5. Jomova, K.; Makova, M.; Alomar, S.Y.; Alwasel, S.H.; Nepovimova, E.; Kuca, K.; Rhodes, C.J.; Valko, M. Essential metals in health and disease. *Chem. Biol. Interact.* **2022**, *367*, 110173. [[CrossRef](#)]
6. Lovell, M.; Robertson, J.; Teesdale, W.; Campbell, J.; Markesbery, W. Copper, iron and zinc in Alzheimer's disease senile plaques. *J. Neurol. Sci.* **1998**, *158*, 47–52. [[CrossRef](#)] [[PubMed](#)]
7. Khan, H.; Tundis, R.; Ullah, H.; Aschner, M.; Belwal, T.; Mirzaei, H.; Akkol, E.K. Flavonoids targeting NRF2 in neurodegenerative disorders. *Food Chem. Toxicol.* **2020**, *146*, 111817. [[CrossRef](#)] [[PubMed](#)]

8. Gnegy, M.E. Catecholamines. In *Basic Neurochemistry*, 8th ed.; Brady, S.T., Siegel, G.J., Albers, W.R., Price, D.L., Eds.; Elsevier Inc.: Amsterdam, The Netherlands, 2012; pp. 283–299.
9. Felten, D.; O'Banion, M.; Maida, M. Neurons and Their Properties. In *Netter's Atlas of Neuroscience*, 3rd ed.; Elsevier Inc.: Amsterdam, The Netherlands, 2016; pp. 1–42.
10. Nagatsu, T.; Sawada, M. L-dopa therapy for Parkinson's disease: Past, present, and future. *Park. Relat. Disord.* **2009**, *15*, S3–S8. [[CrossRef](#)]
11. Eisenhofer, G.; Lenders, J.W.M. Catecholamines. In *Encyclopedia of Endocrine Diseases*, 2nd ed.; Huhtaniemi, I., Martini, L., Eds.; Elsevier Inc.: Amsterdam, The Netherlands, 2018; pp. 21–24.
12. Howes, O.; Kapur, S. The Dopamine Hypothesis of Schizophrenia: Version III—The Final Common Pathway. *Schizophr. Bull.* **2009**, *35*, 549–562. [[CrossRef](#)]
13. García, C.R.; Angelé-Martínez, C.; Wilkes, J.A.; Wang, H.C.; Battin, E.E.; Brumaghim, J.L. Prevention of iron- and copper-mediated DNA damage by catecholamine and amino acid neurotransmitters, L-DOPA, and curcumin: Metal binding as a general antioxidant mechanism. *Dalt. Trans.* **2012**, *41*, 6458–6467. [[CrossRef](#)]
14. Napolitano, A.; Manini, P.; d'Ischia, M. Oxidation Chemistry of Catecholamines and Neuronal Degeneration: An Update. *Curr. Med. Chem.* **2011**, *18*, 1832–1845. [[CrossRef](#)] [[PubMed](#)]
15. Adolfsson, R.; Gottfries, C.G.; Roos, B.E.; Winblad, B.; Gartner, J.; Langford, A.; O'Brien, A.; Hosang, G.M.; Fisher, H.L.; Hodgson, K.; et al. Changes in the Brain Catecholamines in Patients with Dementia of Alzheimer Type. *Br. J. Psychiatry* **1979**, *135*, 216–223. [[CrossRef](#)] [[PubMed](#)]
16. Jomova, K.; Vondrakova, D.; Lawson, M.; Valko, M. Metals, oxidative stress and neurodegenerative disorders. *Mol. Cell. Biochem.* **2010**, *345*, 91–104. [[CrossRef](#)] [[PubMed](#)]
17. Walaas, E.; Walaas, O.; Haavaldsen, S.; Pedersen, B. Spectrophotometric and electron-spin resonance studies of complexes of catecholamines with Cu(II) ions and the interaction of ceruloplasmin with catecholamines. *Arch. Biochem. Biophys.* **1963**, *100*, 97–109. [[CrossRef](#)] [[PubMed](#)]
18. Fazakerley, G.V.; Linder, P.W.; Torrington, R.G.; Wright, M.R.W. Potentiometric and spectrophotometric studies of the copper(II) complexes of methyl dopa, methyltyrosine, and catechol in aqueous solution. *J. Chem. Soc. Dalton Trans.* **1979**, *12*, 1872–1880. [[CrossRef](#)]
19. Fujisawa, K.; Ono, T.; Okamura, M. Synthesis and Characterization of Catecholato Copper(II) Complexes with Sterically Hindered Neutral and Anionic N3 Type Ligands: Tris(3,5-diisopropyl-1-pyrazolyl)methane and Hydrotris(3,5-diisopropyl-1-pyrazolyl)borate. *Inorganics* **2020**, *8*, 37. [[CrossRef](#)]
20. Padnya, P.; Shibaeva, K.; Arsenyev, M.; Baryshnikova, S.; Terenteva, O.; Shiabiev, I.; Khannanov, A.; Boldyrev, A.; Gerasimov, A.; Grishaev, D.; et al. Catechol-Containing Schiff Bases on Thiocalixarene: Synthesis, Copper (II) Recognition, and Formation of Organic-Inorganic Copper-Based Materials. *Molecules* **2021**, *26*, 2334. [[CrossRef](#)] [[PubMed](#)]
21. Kalinowska, M.; Gryko, K.; Gołębiewska, E.; Świdorski, G.; Lewandowska, H.; Pruszyński, M.; Zawadzka, M.; Kozłowski, M.; Sienkiewicz-Gromiuk, J.; Lewandowski, W. Fe(III) and Cu(II) Complexes of Chlorogenic Acid: Spectroscopic, Thermal, Anti-/Pro-Oxidant, and Cytotoxic Studies. *Materials* **2022**, *15*, 6832. [[CrossRef](#)]
22. Kostrzewa, R.M.; Kostrzewa, J.P.; Brus, R. Neuroprotective and neurotoxic roles of levodopa (L-DOPA) in neurodegenerative disorders relating to Parkinson's disease. *Amino Acids* **2002**, *23*, 57–63. [[CrossRef](#)]
23. Valko, M.; Morris, H.; Cronin, M.T.D. Metals, Toxicity and Oxidative Stress. *Curr. Med. Chem.* **2005**, *12*, 1161–1208. [[CrossRef](#)] [[PubMed](#)]
24. Pardo, B.; Mena, M.A.; Fahn, S.; de Yébenes, J.G. Ascorbic acid protects against levodopa-induced neurotoxicity on a catecholamine-rich human neuroblastoma cell line. *Mov. Disord.* **1993**, *8*, 278–284. [[CrossRef](#)] [[PubMed](#)]
25. Baez, S.; Segura-Aguilar, J.; Widersten, M.; Johansson, A.S.; Mannervik, B. Glutathione transferases catalyse the detoxication of oxidized metabolites (o-quinones) of catecholamines and may serve as an antioxidant system preventing degenerative cellular processes. *Biochem. J.* **1997**, *324*, 25–28. [[CrossRef](#)] [[PubMed](#)]
26. Paris, I.; Dagnino-Subiabre, A.; Marcelain, K.; Bennett, L.B.; Caviedes, P.; Caviedes, R.; Azar, C.O.; Segura-Aguilar, J. Copper neurotoxicity is dependent on dopamine-mediated copper uptake and one-electron reduction of aminochrome in a rat substantia nigra neuronal cell line. *J. Neurochem.* **2001**, *77*, 519–529. [[CrossRef](#)] [[PubMed](#)]
27. Boggess, R.K.; Martin, R.B. Copper(II) Chelation by Dopa, Epinephrine, and Other Catechols. *J. Am. Chem. Soc.* **1975**, *97*, 3076–3081. [[CrossRef](#)]
28. West, G.B. Oxidation of adrenaline in alkaline solution. *Br. J. Pharmacol. Chemother.* **1947**, *2*, 121–130. [[CrossRef](#)]
29. Trautner, E.M.; Bradley, T.R. The Early Stages of the Oxidation of Adrenaline in Dilute Solution. *Aust. J. Biol. Sci.* **1951**, *4*, 303–343. [[CrossRef](#)]
30. Balla, J.; Kiss, T.; Jameson, R.F. Copper(II)-catalyzed oxidation of catechol by molecular oxygen in aqueous solution. *Inorg. Chem.* **1992**, *31*, 58–62. [[CrossRef](#)]
31. Jomova, K.; Hudecova, L.; Lauro, P.; Simunková, M.; Barbierikova, Z.; Malcek, M.; Alwasel, S.H.; Alhazza, I.M.; Rhodes, C.J.; Valko, M. The effect of Luteolin on DNA damage mediated by a copper catalyzed Fenton reaction. *J. Inorg. Biochem.* **2022**, *226*, 111635. [[CrossRef](#)] [[PubMed](#)]
32. Dimić, D.; Milenković, D.; Dimitrić Marković, J.; Marković, Z. Antiradical activity of catecholamines and metabolites of dopamine: Theoretical and experimental study. *Phys. Chem. Chem. Phys.* **2017**, *19*, 12970–12980. [[CrossRef](#)]

33. Kładna, A.; Berczyński, P.; Kruk, I.; Michalska, T.; Aboul-Enein, H.Y. Scavenging of hydroxyl radical by catecholamines. *Luminescence* **2012**, *27*, 473–477. [[CrossRef](#)]
34. Kładna, A.; Berczyński, P.; Kruk, I.; Michalska, T.; Aboul-Enein, H.Y. Superoxide anion radical scavenging property of catecholamines. *Luminescence* **2013**, *28*, 450–455. [[CrossRef](#)]
35. Bindoli, A.; Scutari, G.; Rigobello, M.P. The role of adrenochrome in stimulating the oxidation of catecholamines. *Neurotox. Res.* **1999**, *1*, 71–80. [[CrossRef](#)]
36. Simunkova, M.; Barbierikova, Z.; Jomova, K.; Hudcová, L.; Lauro, P.; Alwasel, S.H.; Alhazza, I.; Rhodes, C.J.; Valko, M. Antioxidant vs. Prooxidant Properties of the Flavonoid, Kaempferol, in the Presence of Cu (II) Ions: A ROS-Scavenging Activity, Fenton Reaction and DNA Damage Study. *Int. J. Mol. Sci.* **2021**, *22*, 1619. [[CrossRef](#)]
37. Firme, C.L.; Antunes, O.A.C.; Esteves, P.M. Relation between bond order and delocalization index of QTAIM. *Chem. Phys. Lett.* **2009**, *468*, 129–133. [[CrossRef](#)]
38. Wu, J.; Yu, D.; Liu, S.; Rong, C.; Zhong, A.; Chattaraj, P.K.; Liu, S. Is It Possible to Determine Oxidation States for Atoms in Molecules Using Density-Based Quantities? An Information-Theoretic Approach and Conceptual Density Functional Theory Study. *J. Phys. Chem. A* **2019**, *123*, 6751–6760. [[CrossRef](#)]
39. Ferreira, C.M.H.; Pinto, I.S.S.; Soares, E.V.; Soares, H.M.V.M. (Un)suitability of the use of pH buffers in biological, biochemical and environmental studies and their interaction with metal ions—a review. *RSC Adv.* **2015**, *5*, 30989–31003. [[CrossRef](#)]
40. Mash, H.E.; Chin, Y.P.; Sigg, L.; Hari, R.; Xue, H. Complexation of copper by zwitterionic aminosulfonic (good) buffers. *Anal. Chem.* **2003**, *75*, 671–677. [[CrossRef](#)] [[PubMed](#)]
41. Stoll, S.; Schweiger, A. EasySpin, a comprehensive software package for spectral simulation and analysis in EPR. *J. Magn. Reson.* **2006**, *178*, 42–55. [[CrossRef](#)] [[PubMed](#)]
42. Becke, A.D. Density-functional exchange-energy approximation with correct asymptotic behavior. *Phys. Rev. A* **1988**, *38*, 3098–3100. [[CrossRef](#)] [[PubMed](#)]
43. Lee, C.; Yang, W.; Parr, R.G. Development of the Colle-Salvetti Correlation-Energy Formula into a Functional of the Electron Density. *Phys. Rev. B* **1988**, *37*, 785–789. [[CrossRef](#)]
44. Vosko, S.H.; Wilk, L.; Nusair, M. Accurate spin-dependent electron liquid correlation energies for local spin density calculations: A critical analysis. *Can. J. Phys.* **1980**, *58*, 1200–1211. [[CrossRef](#)]
45. Becke, A.D. Density-functional thermochemistry. III. The role of exact exchange. *J. Chem. Phys.* **1993**, *98*, 5648. [[CrossRef](#)]
46. McLean, A.D.; Chandler, G.S. Contracted Gaussian basis sets for molecular calculations. I. Second row atoms, Z=11–18. *J. Chem. Phys.* **1980**, *72*, 5639–5648. [[CrossRef](#)]
47. Krishnan, R.; Binkley, J.S.; Seeger, R.; Pople, J.A. Self-consistent molecular orbital methods. XX. A basis set for correlated wave functions. *J. Chem. Phys.* **1980**, *72*, 650–654. [[CrossRef](#)]
48. Wachters, A.J.H. Gaussian Basis Set for Molecular Wavefunctions Containing Third-Row Atoms. *J. Chem. Phys.* **1970**, *52*, 1033–1036. [[CrossRef](#)]
49. Frisch, M.J.; Trucks, G.W.; Schlegel, H.B.; Scuseria, G.E.; Robb, M.A.; Cheeseman, J.R.; Scalmani, G.; Barone, V.; Petersson, G.A.; Nakatsuji, H.; et al. *Gaussian 16, Revision C.01*; Gaussian Inc.: Wallingford, CT, USA, 2016.
50. Bacskay, G.B. A quadratically convergent hartree-fock (QC-SCF) method. Application to open shell orbital optimization and coupled perturbed hartree-fock calculations. *Chem. Phys.* **1952**, *65*, 383–396. [[CrossRef](#)]
51. Miertus, S.; Scrocco, E.; Tomasi, J. Electrostatic Interaction of a Solute with a Continuum. A Direct Utilization of ab Initio Molecular Potentials for the Prediction of Solvent Effects. *Chem. Phys.* **1981**, *55*, 117–129. [[CrossRef](#)]
52. Tomasi, J.; Mennucci, B.; Cammi, R. Quantum Mechanical Continuum Solvation Models. *Chem. Rev.* **2005**, *105*, 2999–3093. [[CrossRef](#)]
53. Bader, R.F.W. *Atoms in Molecules: A Quantum Theory*; Oxford University Press: Oxford, UK, 1990; ISBN 0198558651.
54. Keith, T.A. *AIMAll, Version 14.04.17*, TK Gristmill Software: Overland Park, KS, USA, 2014. Available online: aim.tkgristmill.com (accessed on 1 March 2021).
55. Ai-Guo, Z. Dissecting the nature of halogen bonding interactions from energy decomposition and wavefunction analysis. *Mon. Für Chem.-Chem. Mon.* **2017**, *148*, 1259–1267. [[CrossRef](#)]
56. Portmann, S.; Luthi, H.P. Molekel: An interactive molecular graphics tool. *Chimia* **2000**, *54*, 766–770. [[CrossRef](#)]

Disclaimer/Publisher’s Note: The statements, opinions and data contained in all publications are solely those of the individual author(s) and contributor(s) and not of MDPI and/or the editor(s). MDPI and/or the editor(s) disclaim responsibility for any injury to people or property resulting from any ideas, methods, instructions or products referred to in the content.